Symmetric Liquid-Liquid Interface with a Nonzero Spontaneous Curvature

F. A. M. Leermakers, P. A. Barneveld, J. Sprakel, and N. A. M. Besseling
Laboratory of Physical Chemistry and Colloid Science, Wageningen University, Dreijenplein 6, 6703 HB, Wageningen, The Netherlands
(Received 11 April 2006; published 10 August 2006)

The curvature dependence of the symmetric interface between two immiscible polymer solutions in a common monomeric solvent is analyzed using a self-consistent field theory. Contrary to symmetry arguments we find that the surface tension depends in first order on a nonzero Tolman length. These interfaces further have a negative mean and a positive Gaussian bending modulus. The finite spontaneous curvature is attributed to the adsorption of the solvent at the interface.

DOI: 10.1103/PhysRevLett.97.066103 PACS numbers: 68.05.−n, 61.25.Hq, 68.03.Cd

Mesoscopic length scales in soft condensed matter are intimately linked to curved interfaces. The interfacial tension γ of a fluid interface in general depends on the curvature. In the context of lipid bilayers Helfrich [1] pointed out that

$$\gamma(J, K) = \gamma(0, 0) - k_c J_0 J + \tfrac{1}{2} k_c J^2 + \bar{k} K. \qquad (1)$$

Here $J = \frac{1}{R_1} + \frac{1}{R_2}$ is the mean curvature and $K = (1/R_1) \times (1/R_2)$ the Gaussian curvature, wherein R_1 and R_2 as the principle radii of curvature of the surface, k_c is the mean and $\bar{k}$ the Gaussian bending modulus. Typically, as, for example, in bilayers, the mean bending modulus is positive. Then J_0 is the optimum curvature of a cylindrically curved interface, and therefore J_0 is known as the spontaneous curvature. Molecularly realistic modeling of self-assembly shows that for lipid bilayers the ground state is flat, i.e., $J_0 = 0$, even for multicomponent systems [2]. One may argue that the system of mutually incompatible amphiphilic components in the bilayer is a possible exception: a lateral interface between the lipid domains can be avoided by assigning each phase to its own membrane face. However, in this case already the flat state ($J = 0$) is symmetry broken and the natural consequence is that $J_0 \neq 0$.

Equation (1) may also be used for interfaces between separated liquids. The coefficient in front of the linear term in J [after normalization with $\gamma(0, 0)$] is often referred to as the Tolman length. In this case it is more natural to expect a nonzero J_0 and thus a nonzero Tolman length, in particular, for interfaces with an intrinsic asymmetry, such as in emulsion systems.

In 1893 van der Waals [3] introduced a molecular model for the interface between two immiscible (monomeric) species. From a mean-field analysis it follows that not far from the critical point the interface has a hyperbolic tangent profile and the interfacial tension is given by $\gamma \propto (\Delta\chi)^{3/2}$. Here $\Delta\chi = \chi - 2 \propto T^c - T$ is a measure for the distance to the critical point (reached at the critical interaction parameter $\chi^c = 2$ or equivalently at the critical temperature $T = T^c$). Within this mean-field model Blokhuis and Bedeaux [4] analyzed the bending moduli and found a negative mean bending modulus $k_c \propto -(\Delta\chi)^{1/2}$, a positive Gaussian bending modulus $\bar{k} \propto (\Delta\chi)^{1/2}$, and $J_0 = 0$. (Here and below all energy units are normalized by the thermal energy $k_B T$.) The absence of a finite Tolman length was attributed to the (component A)-(component B) symmetry, according to which the phases are transformed, one into the other by changing A to B and vice versa. In such a symmetric case it is irrelevant which direction the positive curvature is defined, and therefore the surface tension at $J = 0$ should be an optimum. When k_c is negative (as in this case), the interfacial tension has a maximum at $(J, K) = (0, 0)$ and J_0 is the worst curvature. Nevertheless, we will continue referring to J_0 as the spontaneous curvature.

In this Letter we extend the binary van der Waals model to a ternary system and consider again a fully symmetric case: two equally long polymeric components A_N and B_N that have a solubility gap are mixed with a common monomeric (good) solvent S, such that there is only one nonzero Flory-Huggins interaction parameter $\chi \equiv \chi_{AB}$ that expresses the strength of the nearest-neighbor interactions. By increasing the amount of solvent, it is possible to bring this system toward the critical point, i.e., $\chi^{\mathrm{cr}} = 2/(\varphi N)$, where $\varphi = \varphi_A + \varphi_B$ is the overall polymer volume fraction [5]. If the solvent would distribute homogeneously, we return essentially to the two-component system. However, the solvent accumulates at the interface, simply because the adsorption of solvent screens some of the unfavorable A-B contacts. This adsorption changes the problem in a fundamental way. Below we will demonstrate that in such a symmetric three-component interface J_0 does not vanish. Our conclusion is that the symmetry argument used repeatedly above is flawed.

Dextran and gelatin, both water-soluble biomacromolecules, have a miscibility gap where two aqueous phases separate. Emulsions of these components find applications in food systems. With increasing water content the interfacial tension can become very low and there are speculations for this system about the mechanical parameters [6],

i.e., $k_c \gg 1$. The present model captures the essential equilibrium aspects of these systems and the calculations should therefore give semiquantitative insight in the thermodynamic and mechanical properties of these interfaces.

The model features freely jointed Markov chains on a lattice. The Scheutjens-Fleer self-consistent field theory [7–10] is used to accurately solve for the partition function for various curvatures of the interface. Fitting of the interfacial tension, evaluated at the surface of tension, to Eq. (1) gives access to the mechanical parameters. As usual, the start is the mean-field free energy F which can be expressed as

$$F = -\ln Q([u]) - \sum_r M(r) \sum_i u_i(r)\varphi_i(r) + F^{\text{int}}([\varphi]) + \sum_r u'(r)\Big(\sum_i \varphi_i(r) - 1\Big). \quad (2)$$

Here and below all linear lengths are normalized to the characteristic length in the lattice b, and r is thus a discrete coordinate. $M(r)$ is the number of lattice sites at coordinate r. For the flat interface $M(r) = L^2$, for the cylindrical interface $M(r) \propto Lr$, and for the spherical interface, we use $M(r) \propto r^2$. Typically the number of sites L is chosen large such that end effects can be ignored and the problem reduces to one with segment density gradients in the r direction only. As in the van der Waals model the interaction part to the free energy F^{int} is a function of the volume fractions:

$$F^{\text{int}} = \sum_r M(r)\varphi_A(r)\chi\langle\varphi_B(r) - \varphi_B^b\rangle. \quad (3)$$

The φ^b refers to the volume fraction in bulk which exists at large values of r (far from the interface). The site average, indicated by the angular brackets, accounts for local and nonlocal contributions to the interaction energy and is computed by $\langle X(r)\rangle = \sum_{r'} \lambda_{r'-r}(r)X(r') \approx X(r) + \lambda_1 \nabla_r X(r)$. The *a priori* step probabilities λ are geometry dependent and obey the detailed balance $M(r+1)\lambda_{-1}(r+1) = M(r)\lambda_1(r)$. Moreover, they are normalized $\sum_{r'=r-1,r,r+1} \lambda_{r'-r}(r) = 1$. The fourth term in Eq. (2) decouples the volume fractions of the components $i = A, B, S$, where the Lagrange parameter $u'(r)$ is linked to the incompressibility constraint. The first term of Eq. (2) features the partition function for the (u, V, T) ensemble $Q = \Pi_i \frac{(q_i([u_i]))^{n_i}}{n_i!}$, where q_i is the single chain partition function. Finally, the second term in Eq. (2) is a Legendre transformation such that the first two terms essentially give the dimensionless entropy. The optimization of the free energy leads to the equations

$$\frac{\partial F}{\partial \varphi_i(r)} = -u_i(r) + u'(r) + \chi_{ij}\langle\varphi_j(r) - \varphi_j^b\rangle = 0, \quad (4)$$

$$\frac{\partial F}{\partial u_i(r)} = -\frac{\partial \ln Q}{\partial u_i(r)} - M(r)\varphi_i(r) = 0, \quad (5)$$

$$\frac{\partial F}{\partial u'(r)} = \sum_i \varphi_i(r) - 1 = 0. \quad (6)$$

Here $\chi_{ij} = \chi$ if $i = A$ and $j = B$ or vice versa. An efficient route to compute the partition function starts with the Boltzmann weights $G_i(r) = \exp -u_i(r)$, which are used in the propagator equation

$$G_i(r, s) = G_i(r)\langle G_i(r, s-1)\rangle \quad (7)$$

for $s = 1, \ldots, N_i$, where the angular brackets again indicate a geometry-dependent site averaging. We note that, when in this averaging the summation over r' is replaced by an integration and $G(r', s-1)$ by its Taylor expansion around $G(r, s)$, the well-known Edwards equation is obtained [11]. The propagators (7) are started with $G_i(r, 1) = G_i(r)\ \forall r$ and produces $q_i = \sum_r M(r)G_i(r, N)$. Now Eq. (5) may be used to evaluate the volume fraction profiles. It can be shown that the results are identical to the use of the so-called composition law which combines two subpartition functions:

$$\varphi_i(r) = \frac{n_i}{q_i} \sum_{s=1}^{N_i} \frac{G_i(r, s)G_i(r, N-s+1)}{G_i(r)}. \quad (8)$$

The position of the interface is controlled by the number of A molecules n_A in the system. As the normalization constant $n_A/q_A = \varphi_A^b/N_A$, we have access to φ_A^b. The volume fraction of the solvent in the bulk as an input parameter and Eq. (8) applied for the solvent gives $\varphi_S(r) = \varphi_S^b \exp -u'(r)$. The value of the Lagrange field $u'(r)$ can thus be computed from the distribution of the solvent. From the incompressibility of the bulk we know $\varphi_B^b = 1 - \varphi_A^b - \varphi_S^b$. The distributions of the B components are normalized by $\varphi_B^b/N_B = n_B/q_B$.

Equations (4)–(6) are solved numerically up to high precision [9]. For the self-consistent solution it is possible to evaluate the grand potential $\Omega = \sum_r M(r)\omega(r)$, where the dimensionless grand potential density is given by

$$\omega(r) = -\sum_i \frac{\varphi_i(r) - \varphi_i^b}{N_i} + \ln\frac{\varphi_S(r)}{\varphi_S^b} - \chi\Big(\frac{\varphi_A(r)\langle\varphi_B(r)\rangle + \varphi_B(r)\langle\varphi_A(r)\rangle}{2} - \varphi_A^b\varphi_B^b\Big). \quad (9)$$

The interfacial tension of the flat interface follows from $\gamma = \sum_z \omega(z)$. The flat interface is fully symmetric, and it is appropriate to place the $z = 0$ at the central plane such that the grand potential density profile obeys $\omega(z) = \omega(-z)$. Of course, $\omega(z)$ is zero far from the interface and peaks at $z = 0$. The three governing parameters (N, χ, and $\varphi \equiv \varphi^b = 1 - \varphi_S^b$) can be used to bring the system closer to the critical point. It is convenient to introduce a reduced interaction parameter $\Delta\chi \equiv N\chi\varphi - 2$ which becomes zero when the system is critical.

It is found (not shown) that the surface tension of the flat interface is given by $\gamma \propto \chi^{1/2}\varphi^{3/2}(\Delta\chi)^{3/2}$ with a numerical coefficient of approximately 40: the surface tension vanishes with the same power law as in the van der Waals model. The profiles of the A component is the mirror-image of that of B. Both profiles are tanhlike. The equimolar planes of A and B do not coincide because the solvent adsorbs at the interface. Below we will discuss this in more detail. The adsorbed amount of solvent vanishes as a power law when the system is taken toward the critical point $\Gamma_S = \sum_z(\varphi_S(z) - \varphi_S^b) \propto (\Delta\chi)^{1/2}$. Other results are very similar to those obtained for the van der Waals interface. For example, the width of the interface diverges as $\delta \propto (\Delta\chi)^{-1/2}$ and the volume fraction difference between the two phases $\propto 1/\delta$.

Figure 1 collects typical results for a curved interface wherein the interface is placed at $r \approx 50$ for the case that $\Delta\chi = 1$. In this example the volume fraction of solvent $\varphi_S^b = 0.8$. Figure 1(a) gives the radial volume fraction profiles of the A and B units, which are both tanhlike. Because of the curvature, the system is somewhat over saturated by A units (Kelvin effect) and the volume fraction profiles are not fully symmetric. Also the distribution of the solvent, as shown in 1(b), is affected by the curvature. It is important to mention that the adsorption of solvent at the interface is significant. In the interfacial zone, $\varphi_S(r) > \varphi_S^b$. As can be seen from Fig. 1(c) the curved interface is accompanied by a well-defined Laplace pressure $\Delta P = -\omega(0)$ and the grand potential density has (as in the flat case) a pronounced maximum in the interfacial zone. All these results are well known [12].

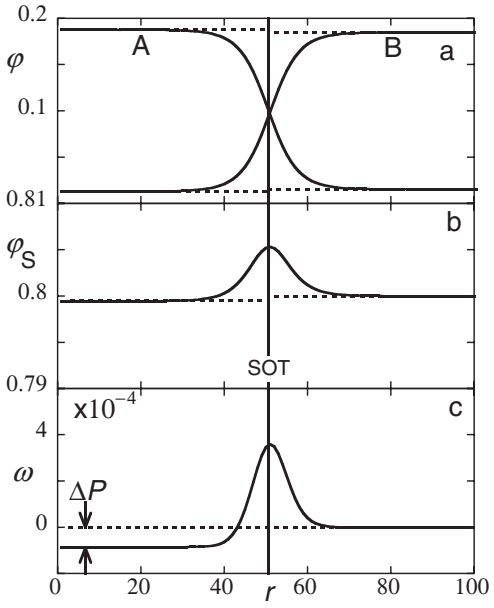

FIG. 1. (a) The volume fraction profile of the A and B units across the cylindrically curved interface for the case that there are 33 molecules of A per unit length in the system. (b) The volume fraction profile of the solvent molecules when $\varphi_S^b = 0.8$. (c) The corresponding dimensionless grand potential density profile across the interface. Parameters $N = 100$, $\chi = 0.15$, and thus $\Delta\chi = 1$. The vertical line is plotted at the radius of tension. The horizontal dotted lines are drawn to help identify the Laplace pressure ΔP and the differences in composition between the inside and outside of the droplet. The surface tension is $\gamma_{\mathrm{SOT}} = 0.004\,269$.

Much is known about the physics of curved interfaces [12]. The grand potential $\Omega = -\Delta PV + \gamma A$. Both the area A as well as the volume V of the internal phase depend on the choice where exactly the radius R is placed. As Ω and ΔP are unambiguously defined, it turns out that γ is a function of the *choice* of R. There exists a special radius for which $[\partial\gamma/\partial R] = 0$, where the square brackets indicate that we consider the variation of γ upon a variation of the choice of R. This position is called the surface of tension (SOT). For example, for the cylindrical interface the SOT is exactly at $R_{\mathrm{SOT}} = \sqrt{\Omega/(\pi\Delta P)}$, and the vertical line in Fig. 1 is drawn at this value of r. Below we report the surface tensions evaluated at the surface of tension. Close inspection of Fig. 1 proves that the SOT does not coincide with the peak of the solvent profile. However, in the limit of $J \to 0$ the SOT exactly goes to the symmetry point $\varphi_A(r) = \varphi_B(r)$.

In Fig. 2 we present the surface tension as a function of the imposed curvature J of both spherically as well as cylindrically curved interfaces. Equation (1) is used to fit the numerical data. For the example of Fig. 2 the result is that $k_c = -0.136$, the Gaussian bending modulus $\bar{k} = 0.021$, and the spontaneous curvature $J_0 = 0.009\,79$ (the latter result is found for both fits), implying a finite Tolman length ($\frac{k_c J_0}{\gamma(0,0)}$): consistent with a finite difference between the SOT and the equimolar planes [13]. The sign of the curvature is quite arbitrarily chosen with respect to the curvature toward the A-rich phase. We could have chosen to count the positive curvature oppositely. As a result, the

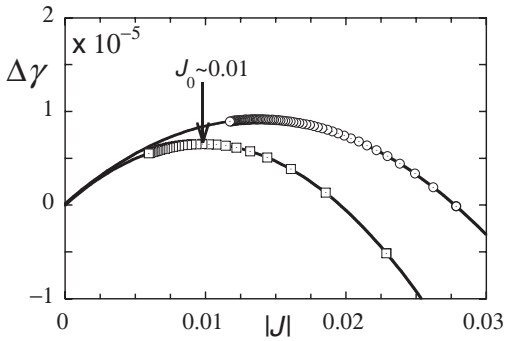

FIG. 2. The surface tension (evaluated at the surface of tension) reduced with that of the flat interface $\Delta\gamma = \gamma_{\mathrm{SOT}}(J, K) - \gamma(0, 0)$ is plotted as a function of the curvature $J = 1/R_{\mathrm{SOT}}$ in the cylindrical shaped (squares) interface or $J = 2/R_{\mathrm{SOT}}$ in the spherically curve (circles) interface. Parameters as in Fig. 1. As the same curve is found for negative curvatures, we present the result as a function of the absolute value $|J|$.

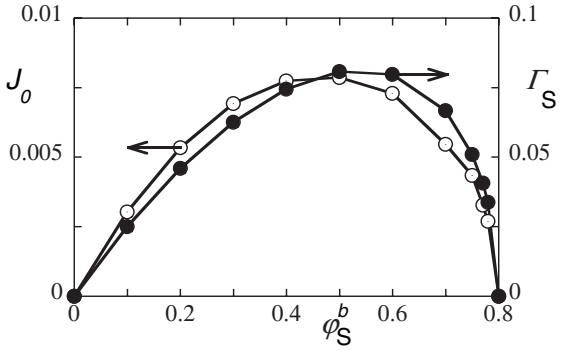

FIG. 3 (color online). The spontaneous curvature J_0 in units b^{-1} (left ordinate) and the adsorbed amount of solvent Γ_S at the flat interface in units b^{-2} as a function of the volume fraction of solvent S in the bulk. Parameters $N = 100$ and $\chi = 0.1$.

same curve is found for the negative values of J, and therefore we have plotted the result in Fig. 2 using the absolute value of J. As a result, at $J = 0$ the surface tension has two distinct derivatives $(\partial\gamma/\partial J)_{J\downarrow 0} = -(\partial\gamma/\partial J)_{J\uparrow 0}$. In the symmetry argument used above, one erroneously assumed that $\partial\gamma/\partial J$ is well defined at $J = 0$.

The result of Fig. 3 may be used to explain why there is a nonzero spontaneous curvature in this symmetric interface. In this figure we show the correlation between the spontaneous curvature and the adsorbed amount of solvent at the interface; both quantities are plotted as a function of φ_S^b. In the absence of solvent, i.e., $\varphi_S^b = 0$, we return to a two-component system and the spontaneous curvature (and obviously also the adsorbed amount) is zero. For this system the Tolman length is zero; the SOT coincides with the equimolar Gibbs plane. We repeated the calculations for various values of the governing parameters and found that for $\Delta\chi < 1$ the mean bending modulus scales as $k_c \propto -(\Delta\chi)^{1/2}$ and also the Gaussian bending modulus scales as $\bar{k} \propto (\Delta\chi)^{1/2}$ as it did for the simple binary system [4]. In line with results of Fig. 3 for $\varphi_S^b > 0.7$ the spontaneous curvature also vanishes as a power law $J_0 \propto (\Delta\chi)^{1/2}$. In line with this the adsorbed amount vanish as well at $\varphi_S^b = 0.8$ (critical point for the system with $N = 100$ and $\chi = 0.1$). The latter is expected, because when the interface disappears there is nothing to adsorb onto. As a result, both J_0 as well as the adsorbed amount Γ_S go trough a maximum as a function of φ_S^b, and this occurs approximately at $\varphi_S^b \approx 0.5$: indeed J_0 and Γ_S are fundamentally coupled.

In the three-component system we can define one equimolar plane for the A component and one for the B component. The finite adsorption of solvent at the interface causes the two equimolar planes to be at different positions. Above it was mentioned that the SOT is, in the limit of zero curvature, exactly halfway in between the two Gibbs planes. The excess adsorptions counted with respect to the SOT obey in the limit $J \to 0$ to $\Gamma_A^{(\mathrm{SOT})} = \Gamma_B^{(\mathrm{SOT})} = -\frac{1}{2}\Gamma_S^{(\mathrm{SOT})}$. From this it is clear that the distances of the equimolar planes to the SOT is exactly determined by the adsorption of the solvent in the interface, explaining the correlation between a finite J_0 and a nonzero Γ_S.

In the above Helfrich analysis, the bending moduli as well as the spontaneous curvature in a system are determined by fitting $\gamma(J, K)$ to Eq. (1), while the volume fraction of solvent in the bulk is fixed. Of course the solvent concentration in the bulk is a free variable, but in experiments it may not always be easy to control this. For this reason we performed similar calculations in which not the volume fraction of solvent but rather the chemical potential of solvent $\mu_S \equiv \mu_S - \mu_S^{\#}$ was fixed. Indeed, such calculations represent in some subtle way a different experiment. We do not present these results but mention that Fig. 3 is almost quantitatively recovered when the φ_S^b coordinate is replaced by $\exp\mu_S$. This means that the finite spontaneous curvature in these systems cannot be attributed to some subtle constraint in the calculations.

In experimental systems [6] it is likely that there exists some chain length or solvent strength disparity, and a nonzero spontaneous curvature should be expected already from this intrinsic asymmetry. Our thesis, however, is that a nonzero spontaneous curvature exists even when these trivial differences between the two phases vanish. Our conclusion is therefore that it is dangerous to rely on symmetry arguments in a Helfrich analysis. Lipid bilayers typically have $J_0 = 0$. The reason why this is the case should be reconsidered.

[1] W. Helrich, Z. Naturforsch. **28C**, 693 (1973).
[2] M. M. A. E. Claessens, B. F. van Oort, F. A. M. Leermakers, F. A. Hoekstra, and M. A. Cohen Stuart, Biophys. J. **87**, 3882 (2004).
[3] J. S. Rowlinson, J. Stat. Phys. **20**, 197 (1979).
[4] E. M. Blokhuis and D. Bedeaux, Mol. Phys. **80**, 705 (1993).
[5] P. Flory, *Principles of Polymer Chemistry* (Cornell University Press, Ithaca, NY, 1953).
[6] E. Scholten, L. M. C. Sagis, and E. van der Linden, J. Phys. Chem. B **108**, 12 164 (2004).
[7] G. J. Fleer, M. A. Cohen Stuart, J. M. H. M. Scheutjens, T. Cosgrove, and B. Vincent, *Polymers at Interfaces* (Chapman and Hall, London, 1993).
[8] J. M. H. M. Scheutjens and G. J. Fleer, J. Phys. Chem. **83**, 1619 (1979).
[9] O. A. Evers, J. M. H. M. Scheutjens, and G. J. Fleer, Macromolecules **23**, 5221 (1990).
[10] S. M. Oversteegen, P. A. Barneveld, J. van Male, F. A. M. Leermakers, and J. Lyklema, Phys. Chem. Chem. Phys. **1**, 4987 (1999).
[11] S. F. Edwards, Proc. Phys. Soc. London **85**, 613 (1965).
[12] J. S. Rowlinson and B. Widom, *Molecular Theory of Capillarity* (Clarendon Press, Oxford, 1982).
[13] R. C. Tolman, J. Chem. Phys. **17**, 333 (1949).